Determination of the minimal acoustic signal length for fast-acting control of a liquid-fueled turbulent swirl burner by Wavelet and Fourier transform

G. I. Novotni* and V. Józsa
Budapest University of Technology and Economics, Faculty of Mechanical Engineering, Department of Energy Engineering
H-1111 Budapest, Műegyetem rkp. 3.

Abstract
The acoustical signal of combustion noise is often analyzed spectrally by Fourier or Wavelet transform. The present paper focused on the measurement data of a 15 kW diesel oil-fueled swirl burner at various combustion air flow rates and atomizing air pressures, evaluating straight, transitory, and V-shaped flames. It was concluded that the smallest applicable window size is 64 samples which enables the statistical characterization of the combustion noise. Probability density functions were fitted to the spectrally filtered to analyze stable operating points. In addition, a scale parameter filtering performed to evaluate the representativeness of the data gathered by using different window sizes.

Introduction

Fossil fuel utilization reached 86% a few years ago [1], urgently calling for using alternative energy resources. However, certain applications in the industry and aviation are likely to rely on combustion for several additional decades. The emission standards of NO_x emission is fulfilled by lean combustion systems [2]. The lean flammability limit of hydrocarbons is air-to-fuel equivalence ratio $\lambda = 2$ under atmospheric conditions [3] which is approached in the greatest extent [4]. The importance of combustion noise as a potential signal for online control rises from the fact that convection and reignition of upcoming fuel-air mixture packets is common at high λs. This phenomenon increase in frequency as flame blowout is approached.

The acoustically excited oscillations with positive feedback are called thermoacoustic instabilities which may lead to operational failures in some seconds [5]. Consequently, violent conditions should be detected early and counteracted by actuators to prevent system damage [6]. The overall available time for these acts is within 1 s for military gas turbine engines [7].

Combustion noise is a broadband phenomenon [8]; therefore, blunt peaks are surrounded by high-amplitude frequencies in the neighborhood. However, the combustion chamber may have several eigenfrequencies, which are sharp peaks, and superpose the signal from combustion [9,10]. Nair and Lieuwen concluded that near lean blowout of turbulent methane combustion Fast Fourier Transform (FFT) is outperformed by Wavelet transform (WT) in terms of lean blowout prediction [7]. Following this conclusion, Chaudhuri and Cetegen used WT for blowout analysis of propane-air flame [11].

Every practical signal consists of stochastic and deterministic parts in which finding trends of the latter leads to the understanding of the ongoing process. The result of the broadband behavior, combustion noise is largely stochastic in which deterministic fragments contain information about the operation. Hence, the statistical evaluation of the signal is performed in various ways in the literature. Pagliaroli et al. [12] used probability density functions (PDF) to investigate the pressure time series of a slot burner. Another approach is the calculation of Kurtosis for thermoacoustic instabilities [13]. Noiray and Denisov [10] and Boujo et al. [14] used a spectral bandpass filter for thermoacoustic instability detection as well. This approach is the closest one to the applied methods of the present paper.

The novelty of this paper comes from the combination of spectral analysis and evaluation of PDFs. Namely, the characteristic frequencies are filtered from FFT and WT and PDFs were fitted to the temporal function of the amplitudes to evaluate the evolution of the flame. In addition, the effect of window size on the result was evaluated to find the shortest window for spectral analysis.

Measurement setup

A lean premixed prevaporized (LPP) swirl burner was used for the combustion tests, shown in **Fig. 1**. The utilized fuel was standard diesel oil (EN 590:2014). The central fuel pipe is 0.4 mm in diameter, and the atomizing air enters annularly in a nozzle with 0.8 mm inner and 1.6 mm outer diameter at the tip. The atomizing gauge pressure, p_g, was varied from 0.3 to 1.6 bar in six steps. The burner has fixed 45° swirl vanes, the mixing tube is 75.5 mm long, and its inner diameter is 26.8 mm.

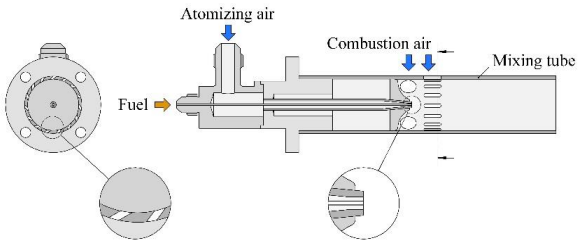

Fig. 1. The used LPP swirl burner.

* Corresponding author: novotni@energia.bme.hu

Fig. 2 shows the measurement setup. The combustion air was delivered by a frequency controlled fan to a preheater. The 400 °C air entered the burner via the swirl vanes and radial holes, shown in **Fig. 1**. The average mixture temperature at the burner discharge varied between 530-590 K, and the average velocity varied from 7.5 to 21.3 m/s, depending on the combustion air flow rate. The estimated Reynolds numbers ranged between 6810 and 18670. In order to improve flame stability, quarls might be applied [15]. Presently, the data of the 15° half cone angle quarl was analyzed since it provided the best overall performance.

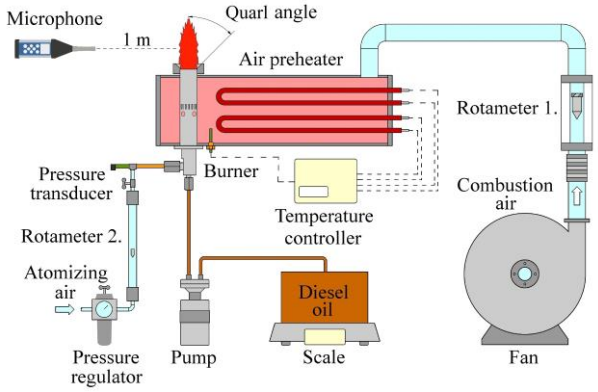

Fig. 2. Measurement setup.

A single measurement started with setting up p_g, then the air mass flow rate was increased from 11.9 kg/h until blowout with 2.38 kg/h steps. Every step was equivalent to a 2 m^3/h air flow rate step on the reading of the rotameter.

For acoustic data sensing and acquisition, a SVAN 971-type noise analyzer was used, placed 1 m from the burner axis. The sampling frequency was 12 kHz which is suitable for detecting combustion noise of turbulent flames [16]. The noise analyzer has a 1/2", 1st class ACO 7052E condenser microphone with a sensitivity of 28.74 mV/Pa. Calibration was performed automatically with an SV33 calibrator (114 dB at 1 kHz, complies with IEC 60942:2003 standard). The raw signal was processed in Matlab. In case of all measurement setups, the recording was continuous. However, at least 20 s data was recorded at each combustion air flow rate after reaching the steady operation.

The investigation regimes started with a straight flame. Due to the fixed swirl vanes, the combustion air flow rate increased the swirl number as well. Therefore, transitory and V-shaped flames were also observed. The estimation of the geometric swirl number, S', was performed, following the work of Beér and Chigier [17]. Straight flame was observed until $S' < 0.41$, the transitory regime was located at $0.41 < S' < 0.82$. Above that, a fully developed V-shaped flame was present.

Methods

The present analysis focuses on the analysis of characteristic frequency bands by using PDFs. The input of the filtering is the amplitude calculated by FFT and WT from various window sizes of steady signals.

A spectrogram which consists of multiple slices of FFT is shown in **Fig. 3**. Shaded areas mark the flame mode change, and black line indicates blowout. The various flame modes feature different typical frequency bands. Straight flame has high-amplitude components in the 3-3.5 kHz regime while V-shaped flames are characterized by bands around 230 Hz and 500 Hz. In the latter case, combustion-related noise is concentrated below 2 kHz compared to the free jet after the blowout. The transitory regime has components from both V-shaped and straight flame frequency bands. The V-shaped spectrum is in line with the finding of Refs. [16,18–20] and it has two, altering peaks [21].

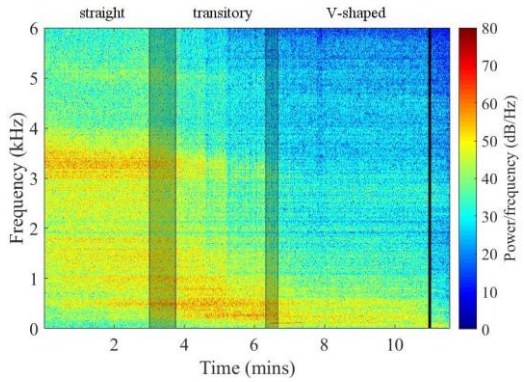

Fig. 3. Spectrogram of 1024 data points with 75% overlapping of a measurement series at p_g = 0.8 bar.

The second analysis method is the WT where the base function is from L^2 space instead of harmonics [22]. The mother wavelet can be developed for an application [7]; however, the use of Morse wavelet for combustion noise was excellent in the present case. The same wavelet was successfully applied by Pawar et al. [23]. Presently, Continuous WT (CWT) was used. Nevertheless, the discrete WT requires less computational effort, CWT enables a more general analysis which leads to input criteria for discrete WT algorithms. The WT is a multiresolution analysis, which means each frequency band has different bandwidth following a geometric series.

Table 1. Center frequencies and bandwidths in Hz of the examined cases, indicating the varying window sizes of the FFT analysis.

Method	CWT	FFT/window size (bandwidth)				
		64	128	256	512	1024
$f_{c,1}$	230.2	187.5 375	187.5 281.6	234.4	234.4	234.4
$b_{c,1}$	16	187.5	93.8	46.9	23.4	11.7
$f_{c,2}$	493.5	562.5	468.8	515.6	492.2	492.2
$b_{c,2}$	34.2	187.5	93.8	46.9	23.4	11.7
$f_{c,3}$	3437	3375	3467	3422	3445	3434
$b_{c,3}$	238.4	187.5	93.8	46.9	23.4	11.7

The filtered center frequencies, f_c, and the corresponding bandwidths, b_cs, are listed in **Table 1** for CWT and FFT. It is the same for CWT for all window sizes, however, it alters with FFT while the bandwidth is also changing. The selected f_cs are the closest to 230, 500,

and 3400 Hz. For FFT with window sizes of 64 and 128 samples, there were two equidistant f_c for 230 Hz. Therefore, both frequencies were noted and analyzed.

The Weibull PDF performed the best in terms of log-likelihood among 20 typical PDFs in engineering practice for all flame modes which was not a trivial result. Therefore, further analysis solely focuses on the use of this PDF.

Figure 4 shows the PDFs in case of linear amplitude values. Three fit parameters, the scale parameter η [dB or Pa/Pa$_{ref}$], shape parameter β [-], and the standard deviation of the PDF, σ [dB or Pa/Pa$_{ref}$], were analyzed in the following parts of the paper. Note that the distribution of **Fig. 4** is similar to the stable pressure time series distribution in Ref. [10].

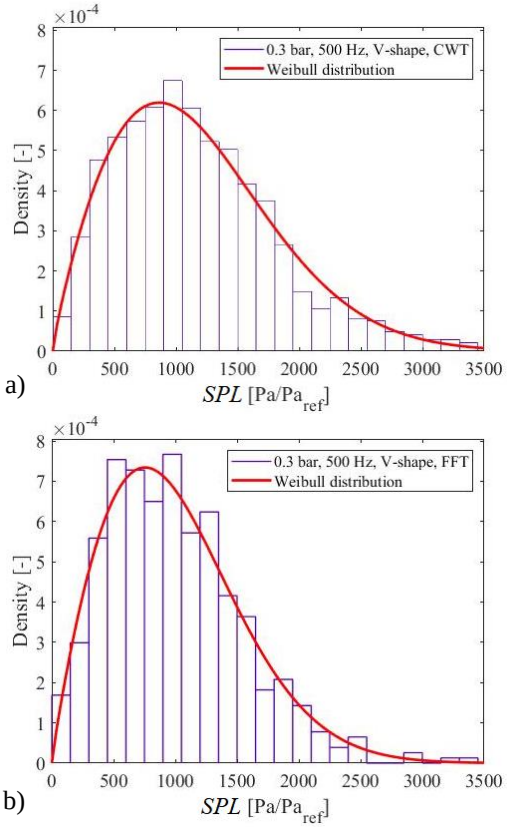

Fig. 4. Fitted PDF using a) CWT and b) FFT of amplitudes at 500 Hz. p_g = 0.3 bar and S' = 1.2.

In the case of CWT, sampling frequency (f_s [Hz]) and sample size (n_s [-]) determined the sample time of a single plot ($t_s = n_s/f_s$ [s]). The CWT algorithm requires at least $n_s = 2^7$ to determine the wavelet coefficients at 500 Hz and $n_s = 2^8$ for 230 Hz. Therefore, n_s was varied between 2^7-2^{13} for 500 Hz and 3400 Hz and 2^8-2^{13} for 230 Hz.

The window size and the overlap of the signal (which was 75% here) affect the time resolution of the available *SPL* at a fixed frequency which equals to the sample size, t_s, when there is no overlap. t_s ranged from 11 ms (2^7 samples) to 683 ms (2^{13} samples). This latter sample size was set to remain below 1 s, a goal mentioned by Nair and Lieuwen [7]. Depending on the window size and overlap, the data points for PDF fitting was calculated as:

$$n_{PDF,FFT} = \frac{t_{s,}}{w_{FFT}} \cdot \frac{1}{1-o_{FFT}}, \qquad (1)$$

where $n_{PDF,FFT}$ is the number of data during t_s time, with w_{FFT} window size and o_{FFT} window overlap. At least 8 data points were used to fit PDF, so cases with lower $n_{PDF,\,FFT}$ values were omitted. The sample size modulated by the overlap is referred to as $t_{s,o}$ later.

In the present paper, the steady operation was evaluated, therefore, characteristics of transitions between measurement points are omitted. Since at least 20 s signal was recorded at each point, the effect of t_s on the determination of PDF parameter values can be evaluated. After sweeping through the analyzed signal and performing spectral filtering, the time series of the fitted PDF parameters are evaluated by calculating their relative standard deviation. They are noted as η_{rstd}, β_{rstd}, and σ_{rstd}. Considering that lean operation is the desired operating condition, the results of the V-shaped mode are emphasized. It was found that the relative standard deviation of all parameters follows the same trend for all flame modes. In the case of V-shaped flames, their relative standard deviations were between 3-10%.

The focus of the present paper is minimizing the relative standard deviation of the PDF parameters while keeping the sampling time low as well. Theoretically, it is the determination of the minimum sample length which provides representative information of the long-term signal properties.

The first task is information collection about the average PDF parameter values to evaluate the properties of the given operating point. This averaging time was varied and referred to as t_{avg} later. Its investigated range was 0.25-2.5 s. Data is available in each $t_{s,o}$ intervals since overlapping is applied. Since the variation of the PDF parameters was high in all cases, a further empirical filtering function, *f*, was used which is de deviation from the average values. Presently, its effect on the results was evaluated in the range of 1-10%. After filtering the PDF parameters, the relative standard deviation was also determined, noted with η_{rstd}', β_{rstd}' and σ_{rstd}'. Another result of the filtering was the average time interval of available data, t', calculated by Eq. (2):

$$t' = \frac{n(t_{s,o})}{n(t_{avg},f)} \cdot t_{s,o}, \qquad (2)$$

where $n(t_{s,o})$ is the number of data points during an examined period, using overlapping, $n(t_{avg}, f)$ is the number of remaining data after filtering, using a t_{avg} data set.

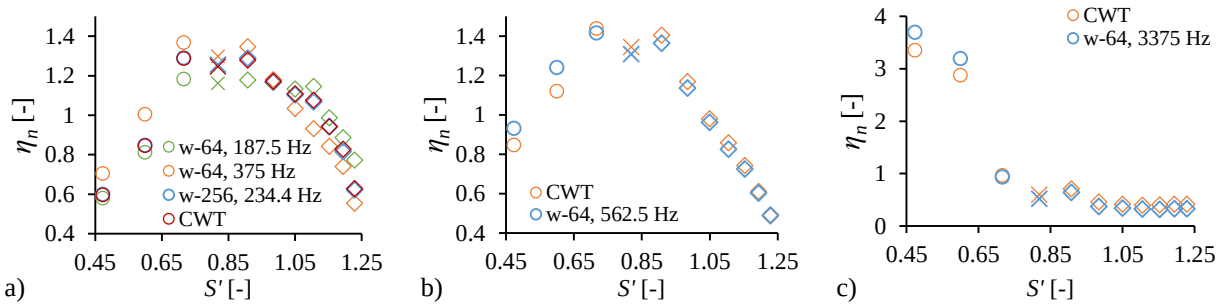

Fig. 5. Normalized scale parameters at a) 230 Hz , b) 500 Hz, and c) 3400 Hz. p_g = 0.3 bar. w-x is the window size of x for FFT. Symbols: straight flame (○), transitory flame (×), and V-shaped flame (◊).

Results and discussion

Figure 5 shows the normalized scale parameter values in case of FFT and CWT methods to the overall average value, using that of the analyzed signal regimes, not the full signal containing transitory regimes between measurement points. At 500 Hz and 3400 Hz, the CWT and FFT results are close to each other. As was mentioned above, at w_{FFT} = 64 both with f_c = 187.5 Hz and f_c = 375 Hz are shown, since the desired 230 Hz frequency lies between them. w_{FFT} = 256 is included as this and above window sizes have f_c close to 230 Hz. Here, CWT and FFT results are closely equivalent and these trends run between the results of FFT at f_c = 187.5 and 375 Hz. With f_c = 187.5 Hz the average value starts to decrease at higher S' values, however it seems to be a better choice because f_c = 375 Hz is more similar to the 500 Hz values. The 230 Hz and 500 Hz components in **Fig. 5** have similar η values. In the case of 500 Hz, the decrease of scale parameter is steeper, which is more suitable for diagnostic purposes, moreover, this trend was closely linear. In the case of 3400 Hz η is significant mostly in straight flames. The similarity of the CWT and FFT methods shows that 8 data points may be enough to fit a PDF that is representative. Varying t_s and p_g do not affect the normalized characteristics of average PDF parameter values, therefore, the presented trends are excellent representatives of the investigated measurement system.

The reason for the exclusion of β and σ values is that the shape parameter had a nearly constant value for each t_s. Its relative standard deviation, considering all flame shapes, was under 3%. The ratio of σ to η was a constant which varied between 30-45% and 75-95% in the case of CWT and FFT, respectively The higher values correspond to higher t_s.

Fig. 6 shows the η_{rstd} values for 230 Hz and 500 Hz as a function of t_s in the case of CWT and FFT with w_{FFT} = 64. In the cases of w_{FFT} = 64 and w_{FFT}=128 (not shown here), the FFT shows less deviation than CWT at each t_s. The same deviation characterizes CWT at 500 Hz than at 230 Hz at halved t_s. Using FFT, the relative standard deviation is nearly the same for all t_s since FFT has the same resolution at all f_cs. The omitted FFT window sizes follow the same characteristic as w_{FFT} = 64, however, increasing the window size also increases η_{rstd} since the frequency resolution varies while that of CWT remains constant for all window sizes and depends on the frequency instead. The w_{FFT} = 128 case provides lower η_{rstd} than CWT. Nevertheless, larger CWT shows lower η_{rstd} for larger window sizes.

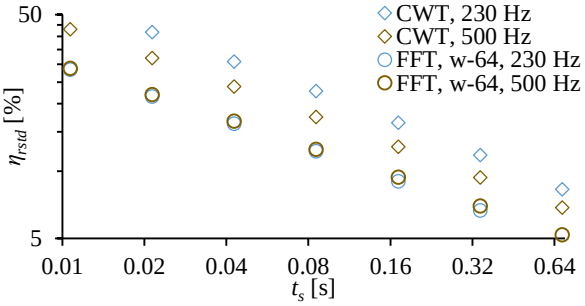

Fig. 6. The relative standard deviation of the scale parameter at 230 and 500 Hz by CWT and FFT at p_g = 0.3 bar. f_c = 187.5 Hz was used for w_{FFT} = 64 samples.

The η_{rstd}' values of V-shaped flame at a given t_{avg} and f showed low sensitivity on S'. Using t_{avg} > 0.5 s and f > 2%, the values at V-shaped flame have an absolute standard deviation between 0.5-1 percent using both CWT and FFT.

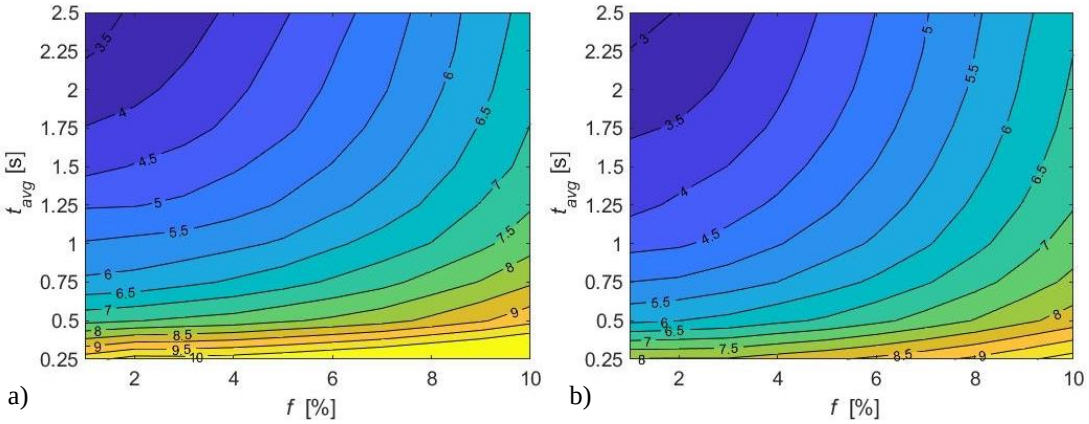

Fig. 7. η_{rstd}' plot at p_g = 0.3 bar by using a) CWT b) FFT with w_{FFT} = 64 of the 500 Hz component.

Figure 7 shows the average of η_{rstd}' as a function of t_{avg} and f at p_g = 0.3 bar in the case of 500 Hz for V-shaped flames. The unfiltered value, η_{rstd} in **Fig. 6** is significantly larger. The results were practically the same for all other w_{FFT} values up to window size of 512. Quantitatively, the deviation of η_{rstd}' was 0.8%, but never exceed 2% of the presented values. The effect of atomization pressure was similar on the average deviation; the maximum value was 3.5%. By comparing the two spectral analyses, the result of FFT showed less η_{rstd}', therefore, it is qualitatively a better method for noise evaluation of turbulent liquid fuel combustion. The averaging time is the governing parameter initially. If the analyzed signal length should remain below 1 s, then the deviation parameter from the average η_{rstd}, f, can be varied without affecting the result in a notable extent. Consequently, the filtering can be adjusted to high f values without altering the results significantly. Therefore, fewer data will be dropped and the result can be determined with higher confidence.

Table 2. t' values in ms corresponding to η in the case of CWT at 500 Hz, p_g = 0.3 bar.

$t_{s,o}$	f [%]									
[ms]	1	2	3	4	5	6	7	8	9	10
3	141	73	49	37	29	24	21	18	16	15
5	214	107	71	54	43	36	31	27	24	22
11	315	160	107	81	65	54	46	41	36	33
21	460	226	152	114	93	78	67	059	53	48
43	677	341	229	172	137	116	100	089	81	74
85	967	487	326	245	200	170	150	135	123	115
171	1285	625	421	324	270	237	216	203	192	185

Table 3. t' values in ms of η in the case of FFT, 500 Hz, w_{FFT} = 64, p_g = 0.3 bar.

$t_{s,o}$	f [%]									
[ms]	1	2	3	4	5	6	7	8	9	10
3	97	49	32	24	19	16	14	12	11	10
5	151	75	49	37	30	25	21	19	17	15
11	220	109	73	55	45	37	32	29	26	23
21	329	165	110	83	67	57	49	44	39	36
43	501	249	166	125	101	86	76	68	63	58
85	711	351	243	187	155	134	120	110	102	97
171	928	461	326	257	222	202	190	181	177	174

Tables 2 and **3** summarizes the filtering process quantitatively for CWT and FFT, respectively. These are containing the t' values for the various t_s and f cases. Modifying t_{avg} did not affect t' values. A notable outcome that even though large window sizes at f = 10% keep all the results, they provided data less frequently than using a significantly reduced window size and dropping out the majority of the calculated data. By quantitatively comparing FFT and CWT, the superiority of the former method is proven in all cases.

The main outcome of this paper was the identification of the governing parameters of combustion noise evaluation. The upcoming tasks are extending the analysis to the transitory regimes where the average moves. In parallel, computational analysis of the code may be performed to find the fastest way for decision making which is the sum of data acquisition and processing times. Following the algorithm for maneuvering, lean blowout evaluation will be also included.

Conclusions

Combustion noise of a 15 kW liquid fueled turbulent burner was evaluated at various swirl numbers and atomization gauge pressures. Each measurement point contained at least 20 s recorded data after reaching steady operation. The microphone data was evaluated by using two spectral techniques, Continuous Wavelet Transform (CWT) and Fast Fourier Transform (FFT). The spectral data at frequencies of 230 Hz, 500 Hz, and 3400 Hz were filtered and evaluated at various window sizes in the case of FFT. The spectrally filtered temporal data was found to follow a Weibull distribution considering all measurement conditions. The scale and shape parameters and the standard deviation of the fitted probability density functions (PDF) were further analyzed. The calculated parameters showed a large relative standard deviation. In order to reduce this value, the data was filtered by an empirical threshold value around the average. The following conclusions were derived:

- FFT showed a lower deviation of PDF fitting parameters compared to CWT at all conditions.
- The fastest sequence of available data after the discussed filtering methods was provided by the shortest reasonable window size, 64 samples, even though the majority of the results are

filtered while nearly all data was usable at large window sizes.
- The empirical threshold of PDF parameter filtering is mostly determined by the sample averaging time below 1 s. It can be concluded that the longer the averaging time the lower the filtered relative standard deviation, hence, the more reliable the result.
- 8 data points of FFT was found to be enough to fit a PDF that represents the combustion noise characteristics.
- Modified relative standard deviation results after filtering around the average value showed low sensitivity on atomizing pressure and sample length, hence, sample size can be as low as 64 to capture the statistical properties of the combustion noise.

Acknowledgments

This paper was supported by the National Research, Development and Innovation Fund of Hungary, project №. OTKA-FK 124704, New National Excellence Program of the Ministry of Human Capacities project №. ÚNKP-18-4-BME-195, Artificial Intelligence research area of Budapest University of Technology and Economics (BME FIKP-MI), and the János Bolyai Research Scholarship of the Hungarian Academy of Sciences.

References

[1] Abas N, Kalair A, Khan N. Review of fossil fuels and future energy technologies. Futures 2015;69:31–49. doi:10.1016/j.futures.2015.03.003.

[2] Correa SM. A Review of NOx Formation Under Gas-Turbine Combustion Conditions. Combust Sci Technol 1993;87:329–62. doi:10.1080/00102209208947221.

[3] Glassman I, Yetter R. Combustion. 4th ed. Burlington: Academic Press; 2008.

[4] Lefebvre AH, Ballal DR. Gas turbine combustion. third. Boca Raton: CRC Press; 2010.

[5] Huang Y, Yang V. Dynamics and stability of lean-premixed swirl-stabilized combustion. Prog Energy Combust Sci 2009;35:293–364. doi:10.1016/j.pecs.2009.01.002.

[6] Ballester J, García-Armingol T. Diagnostic techniques for the monitoring and control of practical flames. Prog Energy Combust Sci 2010;36:375–411. doi:10.1016/j.pecs.2009.11.005.

[7] Nair S, Lieuwen T. Acoustic Detection of Blowout in Premixed Flames. J Propuls Power 2005;21:32–9. doi:10.2514/1.5658.

[8] Strahle WC. Combustion noise. Prog Energy Combust Sci 1978;4:157–76. doi:10.1016/0360-1285(78)90002-3.

[9] Durox D, Moeck JP, Bourgouin JF, Morenton P, Viallon M, Schuller T, et al. Flame dynamics of a variable swirl number system and instability control. Combust Flame 2013;160:1729–42. doi:10.1016/j.combustflame.2013.03.004.

[10] Noiray N, Denisov A. A method to identify thermoacoustic growth rates in combustion chambers from dynamic pressure time series. Proc Combust Inst 2017;36:3843–50. doi:10.1016/j.proci.2016.06.092.

[11] Chaudhuri S, Cetegen BM. Blowoff characteristics of bluff-body stabilized conical premixed flames with upstream spatial mixture gradients and velocity oscillations. Combust Flame 2008;153:616–33. doi:10.1016/j.combustflame.2007.12.008.

[12] Pagliaroli T, Mancinelli M, Troiani G, Iemma U, Camussi R. Fourier and wavelet analyses of intermittent and resonant pressure components in a slot burner. J Sound Vib 2018;413:205–24. doi:10.1016/j.jsv.2017.10.029.

[13] Song WJ, Cha DJ. Temporal kurtosis of dynamic pressure signal as a quantitative measure of combustion instability. Appl Therm Eng 2016;104:577–86. doi:10.1016/j.applthermaleng.2016.05.094.

[14] Boujo E, Denisov A, Bonciolini G, Noiray N, Ebi D. Flame Dynamics Intermittency in the Bistable Region Near a Subcritical Hopf Bifurcation. J Eng Gas Turbines Power 2017;140:061504. doi:10.1115/1.4038326.

[15] Józsa V, Kun-Balog A. Effect of quarls on the blowout stability and emission of pollutants of a liquid-fueled swirl burner. J Eng Gas Turbines Power 2018;140. doi:10.1115/1.4039056.

[16] Singh A V., Yu M, Gupta AK, Bryden KM. Investigation of noise radiation from a swirl stabilized diffusion flame with an array of microphones. Appl Energy 2013;112:313–24. doi:10.1016/j.apenergy.2013.06.034.

[17] Beér JM, Chigier NA. Combustion aerodynamics. London: Robert E. Krieger Publishing Company, Inc.; 1972.

[18] Mahan JR. A Critical Review of Noise Production Models for Turbulent, Gas-Fueled Burners. 1984. doi:10.1039/C5MT00244C.

[19] Kotake S, Takamoto K. Combustion noise: Effects of the shape and size of burner nozzle. J Sound Vib 1987;112:345–54. doi:10.1016/S0022-460X(87)80201-8.

[20] Singh A V., Yu M, Gupta AK, Bryden KM. Thermo-acoustic behavior of a swirl stabilized diffusion flame with heterogeneous sensors. Appl Energy 2013;106:1–16. doi:10.1016/j.apenergy.2013.01.044.

[21] Kumar RN. Further Experimental Results on the Structure and Acoustics of Turbulent Jet Flames. AIAA Pap 1975:483–508. doi:10.2514/5.9781600865176.0483.0507.

[22] Chui CK. An introduction to wavelets. 1st ed. Academic Press; 1992.

[23] Pawar SA, Sujith RI, Emerson B, Lieuwen T. Characterization of forced response of density stratified reacting wake. Chaos 2018;28. doi:10.1063/1.5006453.